AFRPL TR-84-060

AD:

(12)

Final Report
for the period
1 October 1982 to
30 September 1983

A Diffuser Heat Transfer Code

November 1984

Author:
Dr. G. H. Buzzard

Approved for Public Release

**Air Force
Rocket Propulsion
Laboratory**

Air Force Space Technology Center
Space Division, Air Force Systems Command
Edwards Air Force Base,
California 93523-5000

NOTICE

When U.S. Government drawings, specifications, or other data are used for any purpose other than a definitely related government procurement operation, the government thereby incurs no responsibility nor any obligation whatsoever, and the fact that the government may have formulated, furnished, or in any way supplied the said drawings, specifications, or other data, is not to be regarded by implication or otherwise, or conveying any rights or permission to manufacture, use, or sell any patented invention that may in any way be related thereto.

FOREWORD

This final report, A Diffuser Heat Transfer Code, was prepared by Dr Gale H. Buzzard of Duke University during the summer of fiscal year 1983 as an in-house project while serving at the Air Force Rocket Propulsion Laboratory, Edwards Air Force Base, CA, as a visiting professor. The project manager for the Air Force Rocket Propulsion Laboratory was Dr Philip Kessel.

This technical report has been reviewed and is approved for publication and distribution in accordance with the distribution statement on the cover and on the DD Form 1473.

PHILIP A. KESSEL
Project Manager

L. KEVIN SLIMAK
Chief, Interdisciplinary Space Technology Branch

FOR THE DIRECTOR

ROBERT L. GEISLER
Deputy Chief, Propulsion Analysis Branch

SECURITY CLASSIFICATION OF THIS PAGE

REPORT DOCUMENTATION PAGE

1a. REPORT SECURITY CLASSIFICATION: UNCLASSIFIED	1b. RESTRICTIVE MARKINGS
2a. SECURITY CLASSIFICATION AUTHORITY	3. DISTRIBUTION/AVAILABILITY OF REPORT: Approved for Public Release. Distribution Unlimited.
2b. DECLASSIFICATION/DOWNGRADING SCHEDULE	
4. PERFORMING ORGANIZATION REPORT NUMBER(S): AFRPL-TR-84-060	5. MONITORING ORGANIZATION REPORT NUMBER(S)
6a. NAME OF PERFORMING ORGANIZATION: Air Force Rocket Propulsion Lab; 6b. OFFICE SYMBOL (If applicable): DYSO	7a. NAME OF MONITORING ORGANIZATION
6c. ADDRESS (City, State and ZIP Code): Stop 24, Edwards AFB CA 93523-5000	7b. ADDRESS (City, State and ZIP Code)
8a. NAME OF FUNDING/SPONSORING ORGANIZATION; 8b. OFFICE SYMBOL (If applicable)	9. PROCUREMENT INSTRUMENT IDENTIFICATION NUMBER
8c. ADDRESS (City, State and ZIP Code)	10. SOURCE OF FUNDING NOS.

PROGRAM ELEMENT NO.	PROJECT NO.	TASK NO.	WORK UNIT NO
62302F	3148	00	CM

11. TITLE (Include Security Classification): A Diffuser Heat Transfer Code (U)

12. PERSONAL AUTHOR(S): Buzzard, Gale H.

13a. TYPE OF REPORT	13b. TIME COVERED	14. DATE OF REPORT (Yr., Mo., Day)	15. PAGE COUNT
Final	FROM 82/10/1 TO 83/9/30	84/11	49

16. SUPPLEMENTARY NOTATION: Gale H. Buzzard is an assistant professor of Mechanical Engineering at Duke University in Durham, North Carolina.

17 COSATI CODES		
FIELD	GROUP	SUB. GR.
21	08	
21	08	2

18. SUBJECT TERMS (Continue on reverse if necessary and identify by block number): Diffuser Heat Transfer, Two Phase Flows, Particle Impaction, Ground Test Facilities

19. ABSTRACT (Continue on reverse if necessary and identify by block number)

A computer code for diffuser heat transfer analysis (DHT) has been developed which improves upon the earlier Rocket Engine Diffuser Thermal Analysis Program (REDTAP) of Trout and McCay. Improvements contained within DHT include provision for a radial temperature gradient within the diffuser wall, treatment of impingement heat transfer at the point of plume attachment, an improved model for the particle impingement accommodation coefficient, and a model for particle debris shielding.

The 77-inch diffuser located at the Air Force Rocket Propulsion Laboratory was instrumented to record the water side diffuser wall temperature and water jacket temperature at selected sites along the initial seven feet of the diffuser during routine test firings. Comparision of the predictions of DHT and preliminary experimental data show promise but as of the present time inadequate experimental data exist to allow a validation of the code.

20. DISTRIBUTION/AVAILABILITY OF ABSTRACT: UNCLASSIFIED/UNLIMITED ☒ SAME AS RPT. ☐ DTIC USERS ☐	21. ABSTRACT SECURITY CLASSIFICATION: Unclassified
22a. NAME OF RESPONSIBLE INDIVIDUAL: Dr. Phil Kessell	22b. TELEPHONE NUMBER (Include Area Code): (805) 277-5591; 22c. OFFICE SYMBOL: DYSO

DD FORM 1473, 83 APR EDITION OF 1 JAN 73 IS OBSOLETE.

SECURITY CLASSIFICATION OF THIS PAGE

TABLE OF CONTENTS

LIST OF FIGURES

1. INTRODUCTION

A computer program has been developed that performs a thermal analysis of a water jacketed rocket motor test diffuser. The program has been developed to handle the requirements of the particle laden plume associated with a metallized solid propellant but is also capable of handling a particle free plume. The program combines the earlier work of Trout and McCay[1], Pergament[2], and Kessel[3]. The end result is a Diffuser Heat Transfer code (DHT) which corrects several of the shortcomings of the Rocket Engine Thermal Analysis Program (REDTAP) created by Trout and McCay and includes several areas not treated by the earlier code. Included among these areas are radial temperature gradient within the diffuser wall, impingement heat transfer at the point of plume attachment, an improved model for the particle impingement accommodation coefficient, and particle debris shielding.

In addition to the development of the DHT code, the 77-inch diffuser located at the Air Force Rocket Propulsion Laboratory (AFRPL) Test Area 1-42 was instrumented to record water side wall temperature and coolant temperature at selected sites along the initial seven feet of the diffuser during routine test firings. It was anticipated that data would be available early in the project. The principal thrust of the present work was to have been the writing of the DHT code followed by a comparison of the DHT predictions with the experimental data gathered at Test Area 1-42. It was anticipated that the code would evolve as the body of experimental data grew and that the end result would be a diffuser heat transfer code supported by a body of experimental data. Unfortunately, the test firings to date have involved motors that have been too small and/or burn times that have been too short to provide data that are useful in validating the DHT code. The quality of the data thus far has been excellent and there is the promise of useful data at a future date, but much remains to be done in terms of validating the predictions of DHT.

As was the case with the earlier code, DHT relies on the AFRPL Solid Performance Program (SPP)[4] and a modification of the Joint Army Navy NASA Air Force (JANNAF) Standardized Plume Flow Field Model (SCIPPY)[5,6] to provide the flow field data within the diffuser; DHT incorporates the Inter-Agency

Chemical Rocket Propulsion Group Turbulent Boundary Layer code (TBL)[7] as a subroutine to handle the gas side convection heat transfer. Unfortunately, the dependency of DHT upon SCIPPY places a current restriction on the usefulness of DHT. SCIPPY is still in the developmental stage and currently is unable to handle rocket motor/diffuser size combinations that involve large disparities between the exit diameter of the motor and the inlet diameter of the diffuser. Hopefully, as SCIPPY evolves toward its final form, these problems will disappear.

2. STATEMENT OF THE PROBLEM

2.1 GENERAL

The computer code developed and all discussions that follow deal specifically with the 77-inch diffuser located in the AFRPL Test Area 1-42. The code, however, is written to perform a thermal analysis for any similar diffuser and could be easily modified to handle most water jacketed configurations.

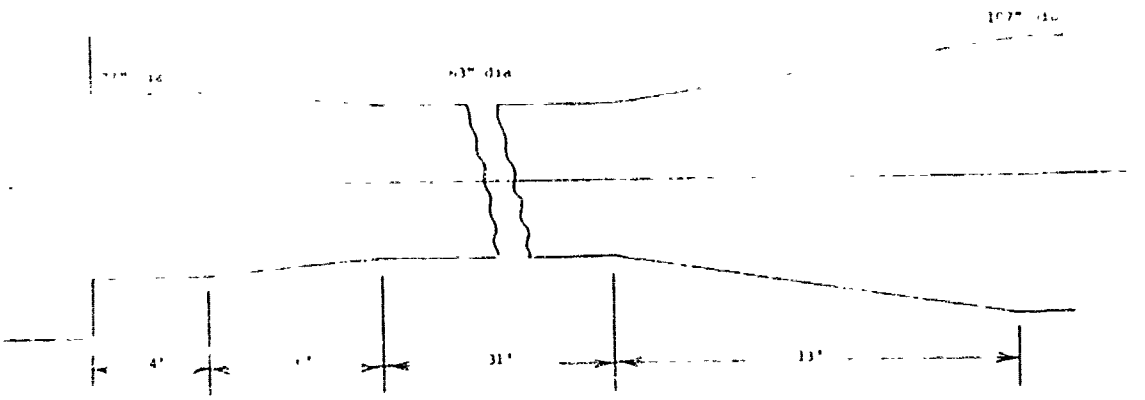

Figure 1. 77" Diffuser, AFRPL Test Area 1-42

Shown in Figure 1 is a schematic of the diffuser. The diffuser has a uniform diameter inlet section followed by a conical transition to a second uniform diameter section and conical expansion. This final expansion connects to a plenum which removes the rocket motor exhaust gases and maintains the reduced pressure necessary to simulate altitude conditions.

The diffuser is fabricated from ASME-SA-285-C steel and has a 0.50-inch inner wall which forms the containment for the exhaust plume. The water jacket is formed by this and a 0.375-inch outer wall. These two walls are separated by 2.5 x 2.5 x 0.5-inch angle wound with a 5.75-inch pitch quadruple lead that results in four parallel coolant passages approximately 5.25 x 2.75

inches. These angle members are welded to the inner wall. No attempt has been made to analyze the thermal path added by these angle members. One can assume that they will provide additional cooling of the inner wall but the extent of this effect is indeterminate. There is the added complication of a nominal 0.25-inch radial clearance between the inner assembly and the outer wall. Since the inner assembly floats within the outer wall, the resulting radial clearance can range from 0 to 0.50 inches. It is assumed that this condition does not short circuit the helical path of the water jacket. This is a question that must be addressed as experimental data become available.

The heat load on the diffuser is comprised of the convective load from the exhaust gases plus the various particle related heat fluxes. The particles carry with them a very significant quantity of thermal energy as a result of their heat capacity and elevated temperature in reference to the gas side wall temperature of the diffuser. They also carry a very significant quantity of kinetic energy. If as they impact the wall, an appreciable portion of either of these energies is transferred to the diffuser wall, a very severe heat load will result. Crucial to a valid diffuser model is the selection or development of a particle impingement model that adequately handles the exchange of these two forms of energy. Radiant exchange from the particles to the wall is a non-negligible but distinctly second order heat load.

The diffuser wall must obey the unsteady heat equation. It is convenient to note that the wall is thin compared with the diffuser radius and to write the heat equation in two-dimensional Cartesian coordinates. As such, the wall temperature is governed by

$$\frac{\partial^2 T}{\partial x^2} + \frac{\partial^2 T}{\partial y^2} = (\rho C/k)\, \partial T/\partial t \qquad (1)$$

where x and y are measured parallel and normal to the diffuser wall and ρ, C and k are the density, specific heat and thermal conductivity of the diffuser wall.

The fluid flow within the water jacket is assumed to be one-dimensional constant property steady flow. It is assumed that the flow rate is known and, therefore, the local fluid velocity is a simple function of the local water jacket cross-sectional area. The temperature distribution within the water

jacket is assumed to be a one-dimensional axial transient superimposed upon the steady flow and involving negligible axial conduction. As such, the water jacket temperature is governed by

$$U \frac{\delta T}{\delta x} + (2 \pi Rh / \rho CA) (T - T_{wall}) = - \delta T / \delta t \qquad (2)$$

where U is the axial velocity of the coolant, R is the outer radius of the inner wall, ρ and C are the density and specific heat of the coolant, A is the axial cross-sectional area of the water jacket, and h is the water side film coefficient. The outer wall of the water jacket is treated as an adiabatic surface. Equations 1 and 2 are solved using explicit finite difference techniques.

2.2. PARTICLE IMPINGEMENT

The aluminum oxide particles contained within the exhaust of a metallized solid propellant rocket motor carry with them a considerable quantity of thermal and kinetic energy. It is convenient to measure the thermal energy relative to the gas side wall temperature of the diffuser and to partition the kinetic energy into a component resulting from the velocity parallel to the diffuser wall and a component resulting from the velocity normal to the wall. In this form the potential heat load caused by the particles impinging on the diffuser wall may be represented by

$$\dot{m}_p C_p (T_p - T_w) + m_p U_p^2/2 + m_p V_p^2/2$$

where $\dot{m}_p$ is the mass flow of particles impinging upon the wall, C_p is the specific heat of the particles, T_p is the temperature of the particle, T_w is the gas side wall temperature of the diffuser, U_p is the velocity of the particle parallel to the wall and V_p is the velocity of the particle normal to the wall.

It is common practice to quantify the particle/wall interaction in terms of three accommodation coefficients (C_T, C_U and C_V) which define the fraction of each energy component that is transferred to the diffuser wall.

Introducing this concept, the heat load on the diffuser wall due to particle impingement is given by the following expression

$$q_{imp} = \dot{m}_p \left[C_T C_p (T_p - T_w) + C_U U_p^2/2 + C_V V_p^2/2 \right] \quad (3)$$

Evaluation of these accommodation coefficients is in large measure a question of particle behavior upon impact with the wall. If the particles adhere to the wall, all three accommodation coefficients are unity and the impingement heat flux will be the dominant heat load on the diffuser. Such an assumption would be a very safe estimate of the maximum heat flux but if overly cautious would preclude the testing of rocket motors that could in reality be safely tested within the facility. Particle impingement with the wall can be expected to occur at a relatively shallow angle. This lends credence to an assumption that the particles do not adhere to the wall and that the thermal accommodation coefficient is close to zero. A further consequence of this assumption would be that the momentum of the particle parallel to the surface, and therefore that component of the kinetic energy, will be conserved. This would lead to a C_U equal to zero. Visual inspection following two Super BATES firings revealed no evidence of significant particle deposition on the diffuser wall.

The transfer of the component of kinetic energy normal to the surface from the particle to the surface can be related to the coefficient of restitution for the collision. After a review of the limited data available, Kessel[3] suggests the use of a coefficient of restitution equal to (1 - B/90), where B is the angle of impact, as measured in degrees, between the velocity vector and the normal to the surface. This leads to the following expressions where V_p is the component of the velocity normal to the surface and the prime denotes conditions following impact.

$$V_p'/V_p = 1 - B/90$$

$$(KE'/KE)_{normal} = (1 - B/90)^2$$

$$(\Delta KE/KE)_{normal} = (B/90)(2 - B/90)$$

The decrease in the normal component of the kinetic energy places an upper bound on the energy transferred to the surface. Unless the particle adheres to the surface, a portion of this energy will be carried away as an increase in the internal energy of the particle. Citing limited data that support an accommodation coefficient of 0.55 to 0.70 for normal impact and noting that the quantity

$$(B/90)(2 - B/90)$$

is approximated within ± 7% by 1.15 SIN B for B less than or equal to 40 degrees, Kessel suggests the use of an accommodation coefficient

$$C_V = 0.8 \text{ SIN } B \qquad (4)$$

The heat load associated with particle impingement is handled within DHT as per Equation 3 with the user allowed to specify any desired set of values for the accommodation coefficients. SCIPPY will provide DHT with local values for B and an option is provided that allows the use of Equation 4 along with the ability to scale the coefficient of SIN B up or down at will. In reporting on data gathered at Arnold Engineering Development Center (AEDC) on an instrumented diffuser, Kessel[3] cites modest agreement between the experimental data and the predictions of REDTAP using accommodation coefficients of 0, 0, and 0.8 SIN B along with a specified average value of B equal to 22 degrees.

2.3 PARTICLE RADIATION

No attempt is made in the present work to alter the radiation model developed within REDTAP by Trout and McCay. This is a very simplistic model that places a believable upper limit on the contribution of particle radiation to the heat load on the diffuser. All particle properties at the exit plane of the rocket motor including particle size are generated by SPP. SPP provides three particle size groups with a very limited amount of size control in the hands of the user. Considerable controversy surrounds the actual size distribution of the particles and whether the three size groups generated by SPP do or do not give an adequate model of the particle flow field. SCIPPY uses the output of SPP to generate the flow field within the diffuser and any shortcomings of SPP in terms of the particle flow field are propagated

throughout the diffuser. SCIPPY in turn introduces its own problems with regard to the particles. If, as discussed in the preceding section, the particles are assumed not to adhere to the wall, they will accumulate as a debris layer along the wall or they will be reentrained within the flow. Within SCIPPY, particles that strike the wall are allowed to pass through the wall and are lost from the flow. In addition, SCIPPY will at some point in the flow drop a Mach disk and will lose all particles which pass through the Mach disk. The radiation heat load is a minor threat to the diffuser and until the particle flow field is better defined a more refined model does not seem justified.

It is assumed that the flow field is optically thin and that the particles behave as gray bodies emitting radiation as per the Stefan-Boltzman equation with all properties evaluated in terms of centerline conditions at the exit plane of the rocket motor. It is further assumed that this emissive power is concentrated as a line source of uniform strength along the centerline of the diffuser. This source strength is readily evaluated in terms of exit plane information from SPP and takes the form

$$q = 3 \dot{m}_p \varepsilon \sigma T_p^4 / U_p \rho_p R_p \tag{5}$$

where σ is the Stefan-Boltzman constant and $\dot{m}_p$ is the mass flow rate, ε the emissivity, T_p the temperature, U_p the axial velocity, ρ_p the mass density, and R_p the particle radius associated with the particle group in question. Equation 5 must be summed over the particle groups present. Defense of this model as used within REDTAP was supported by the assumption of a thermal accommodation coefficient of unity. This resulted in a particle impingement heat load so large as to render the radiation load negligible. With the accommodation coefficients suggested in the present study, the radiation load will become a significant but not major portion of the heat load on the diffuser. On the other hand, the present assumption that the particles do not adhere to the wall lends credence to the assumption of a uniform strength line source of radiation. As a body of experimental data becomes available and a revised SCIPPY provides more reliable flow field data, refinement of this model should be considered.

2.4 GAS SIDE CONVECTION

The gas side convection heat transfer is handled within DHT by incorporating TBL as a subroutine in much the same fashion as was done in REDTAP. SCIPPY provides TBL with the edge conditions for the boundary layer analysis and TBL provides DHT with the film coefficients and adiabatic wall temperatures required for the heat transfer calculation. The boundary layer grows from a stagnation region at the point of plume impingement and therefore it is necessary to start the boundary layer with nonzero initial boundary layer thicknesses. REDTAP started TBL with the initial momentum and energy thicknesses set equal to a single arbitrarily small number. This approach may provide meaningful information well removed from the point of plume impingement but there is no reason to expect it to provide useful film coefficients in the vicinity of plume impingement. Unfortunately, this is probably the most critical region. In addition, no attempt was made to handle the stagnation point heat transfer which occurs at the point impingement. For some cases, this may provide the severest heat load on the diffuser. A more reasonable approach is to evaluate the impingement point heat transfer coefficient independently and to start the boundary layer thicknesses with values that will result in this level of heat transfer. This approach admittedly imposes a boundary layer model on a region that is not a boundary layer flow and one must question the validity of the results immediately downstream of impingement. Preliminary experimental results do, however, show surprisingly good correlation with the predictions of DHT. This is the approach used within DHT and is in essence the approach suggested by Pergament[2].

Pergament cites the work of Donaldson, Snedeker, and Margolis[8] who present data for a 0.511-inch diameter converging nozzle driven by compressed air, discharging to the atmosphere, operationg at pressure ratios of 0.800 to 0.148, and impinging normally upon a flat surface. Donaldson, et al, show correlation between their data and the laminar heat transfer correlation

$$h = k \sqrt{Pr\ (dU/ds)/2\nu} \qquad (6)$$

where H is the film coefficient, k is the thermal conductivity of the gas, Pr is the Prandtl Number of the gas, dU/ds is the velocity gradient of the free stream flow parallel to the surface, and ν is the kinematic viscosity of the

gas--all evaluated just downstream of impingement. The film coefficient as defined by Equation 6 is multiplied by an augmentation factor which ranges from 1.4 to 2.2 and which Donaldson, et al, show to be a function of the distance from the nozzle to the impingement surface and attribute to turbulence growth within the jet prior to impingement.

While there would be no reason to expect the work of Donaldson, et al, to apply directly to the diffuser, there would seem to be hope for using Equation 6 in conjunction with an augmentation factor evolved from experimental diffuser data. The velocity gradient dU/de can be evaluated from velocity data supplied by SCIPPY. While this is an area of the flow that SCIPPY handles rather poorly, the velocity gradient enters as a square root and the associated error is reduced. Preliminary experimental data from two Super BATES firings show good agreement with predictions made using an augmentation factor of 2.5, however, an understanding of this area will come only as we acquire a base of experimental diffuser data.

2.5. DEBRIS LAYER SHIELDING

The assumption that the particles which strike the wall do not adhere to the wall gives rise to an accumulation of these particles in the vicinity of the wall. As this accumulation is swept downstream by the main flow, it will form an increasingly dense sheath of particles adjacent to the wall and will partially shield the wall from particle impingement. Wickman, Mockenhaupt, and Ditore[9] develop a simple model for this phenomenon and present supporting data in conjunction with an erosion study. The essentials of the model are contained in Figure 2. The model assumes a single particle size and a cross sectional area for collision equal to σ. Assuming a particle number density n within the debris layer, the cross-sectional area blocked per unit area by the debris is found to be

$$n\sigma dx / \text{SIN } B.$$

Assuming an incident particle flow with a particle number density of N, the change in particle number density caused by scattering within the debris layer element dx will be

$$dN = N n \sigma dx / \text{SIN } B.$$

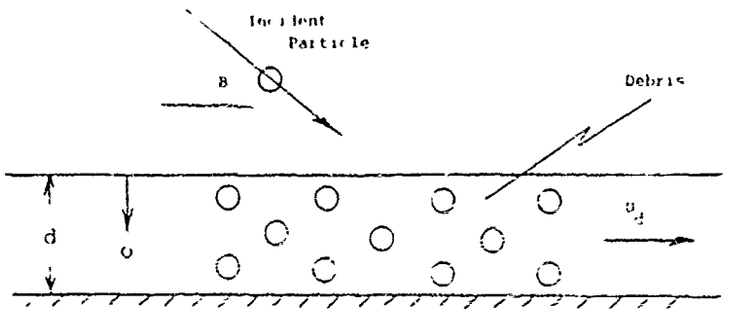

Figure 2. Debris Layer Model.

Collecting like terms and integrating across the debris layer

$$\ln(N_w/N_o) = - c \int_0^d n\, dx \,/\, \text{SIN } \beta \qquad (7)$$

where N_w is the incident particle number density at the wall, N_o is the incident particle number density at the outer edge of the debris layer and their ratic represents the fraction of the incident particles reaching the wall. While neither n nor d is known, the above integral is related to the local mass flow rate of debris through

$$\dot{m}_d = \int_0^d 2\pi R n m_p U_d dx$$

where R is the local diffuser radius, m_p is the particle mass, and U_d is the velocity of the debris. Assuming that the debris is swept along by the edge velocity of the gas, U_g, one can replace U_d with U_g and solve for the integral contained in the above expression as

$$\int_0^d n\, dx = \dot{m}_d / 2\pi R m_p U_g$$

Substituting this expression into Equation 7 one obtains

$$\ln(N_w/N_o) = - \dot{m}_d / 2 \pi R m_p U_g \text{ SIN } B \tag{8}$$

In the case of diffuser flow, m_d is obtained by summing the particle mass flux impinging upstream of the point in question. Information necessary for evaluating everything except σ is available from SCIPPY.

The model just described is readily expanded to include flows involving more than a single size particle. It is convenient to treat each particle size group individually. Assuming three size groups with group j assumed to be the incident particle group and group k the particle debris group, one can consider σ_{jk} as the cross section for particle group j colliding with particle group k, N_j the particle number density of the impinging particles, and n_k the particle number density of the debris. With this nomenclature, Equation 7 may be written as

$$\ln(n_w/N_o)_j = - \sum_{k=1}^{3} \sigma_{jk} \int_0^H n_k dx \; / \; \text{SIN } B_j \tag{9}$$

where H is sufficiently large to include all three debris layers. The right hand side of Equation 9 may be expanded and, noting that as x tends to d, n tends to zero, the upper limit of each integral may be replaced with the individual debris layer thickness, leading to the following form:

$$\ln(N_w/N_o)_j = - \sum_{k=1}^{3} \sigma_{jk} \int_0^{d_k} n_k dx / \text{SIN } B_j . \tag{10}$$

As with Equation 8, it is convenient to recognize that

$$\int_0^d n_k \, dx = \dot{m}_k \; / \; 2 \pi R m_k U_g$$

where $\dot{m}_k$ is the mass flow rate of particle group k within the debris layer and m_k is the mass of a group k particle. Introducing this into Equation 10 leads to

$$\ln(N_w/N_o)_m = - \sum_{k=1}^{3} (\sigma_{jk} \dot{m}_k / m_k) \; / \; 2 \pi R U_g \text{SIN } B_j .$$

Noting that, with the exception of SIN B_j, the above expression is solely a function of the debris layer, it is convenient to define DF, the debris factor, such that

$$\ln(DF_j) = - \sum_{k=1}^{3} (\sigma_{jk} \dot{m}_k / m_k) / 2 \pi R U_g \qquad (11A)$$

and

$$(N_w/N_o) = (DF_j)^{1/SIN\ B_j} \qquad (11B)$$

No mention has been made thus far as to evaluating σ_{jk}. In the development of their particle diameter model, Wickman, et al, assume that any contact at all between impinging particle and debris particle will result in the scattering of the impinging particle. This model leads to

$$\sigma = \pi (2R_p)^2$$

which would appear to be excessive. The model built into DHT assumes that a smaller particle will be scattered by as little as grazing contact, that an equal size particle will require an angle of impact of at least 45 degrees, and that a larger particle must impact a smaller particle with an angle of at least 45 degrees and impact an aggregate mass of such particles equal to its own mass before scattering will occur. This leads to

$$\sigma_{jk} = \begin{cases} \pi (R_j + R_k)^2 & R_j < R_k \\ \pi (R_j + R_k)^2 (R_k/R_j)^3/2 & R_j \geq R_k \end{cases}$$

Introducing this model for σ_{jk} and noting that

$$m_k = 4 \pi R_k^3 \rho_p / 3$$

one is able to evaluate the individual terms of the right hand side of Equation 11A as

$$\sigma_{jk} \dot{m}_k / 2 \pi R U_g m_k = \begin{cases} 3(R_j + R_k)^2 \dot{m}_k / 8 \pi R U_g \rho_p R_k^3 & R_j < R_k \\ 3(R_j + R_k)^2 \dot{m}_k / 16 \pi R U_g \rho_p R_j^3 & R_j \geq R_k \end{cases}$$

The above debris shielding model has been built into DHT and the user is provided with the option to use or not use it in the calculations. If the option is implemented, the particle mass flow rate that appears in Equation 3 will be multiplied by the factor

$$(DF_j)^{1/SIN\ B_j}$$

For the examples looked at to date, debris shielding has not appeared to be a significant factor. The debris factor has ranged from 1.0 to 0.9 but has remained very close to 1.0 in the regions where impingement heating was a major concern. This is understandable since only after particles impinge upon the wall for some distance does the debris layer build up to an effective shield. The reduction of particle mass flux reaching the wall may be as great as 50 percent in some regions but these regions are well downstream of the severe heat load areas. The regions where appreciable debris shielding occurs are where the impingement angle is quite shallow and

$$(DF_j)^{1/SIN\ B_j}$$

can become quite small. For such flows, however, if one is assuming accommodation coefficients of 0, 0, and 0.8 SIN B, the impingement heat load is quite small with or without debris shielding.

2.6 WATER SIDE CONVECTION

The water side film coefficient is evaluated using correlations presented by Marks.[10] The preliminary calculation is handled by

$$h' = 160\ (1 + 0.012\ T_f)\ V^{0.8}/D_h^{0.2} \qquad (13)$$

where T_f is the film temperature of the water measured in degrees Fahrenheit, V is the velocity of the water measured in feet per second, D_h is the hydraulic diameter (4 x area / perimeter) of the channel measured in inches, and h' is the film coefficient measured in $B/hr\text{-}ft^2\text{-}F$. This value for h is modified to compensate for the radius of curvature of the channel ($D_c/2$) such that

$$h = (1 + 3.5\ (D_h/D_c))\ h'. \qquad (14)$$

3. NUMERICAL ANALYSIS

Figure 3 shows the finite difference grid that is used in solving for the temperature distribution within the diffuser wall and the water jacket.

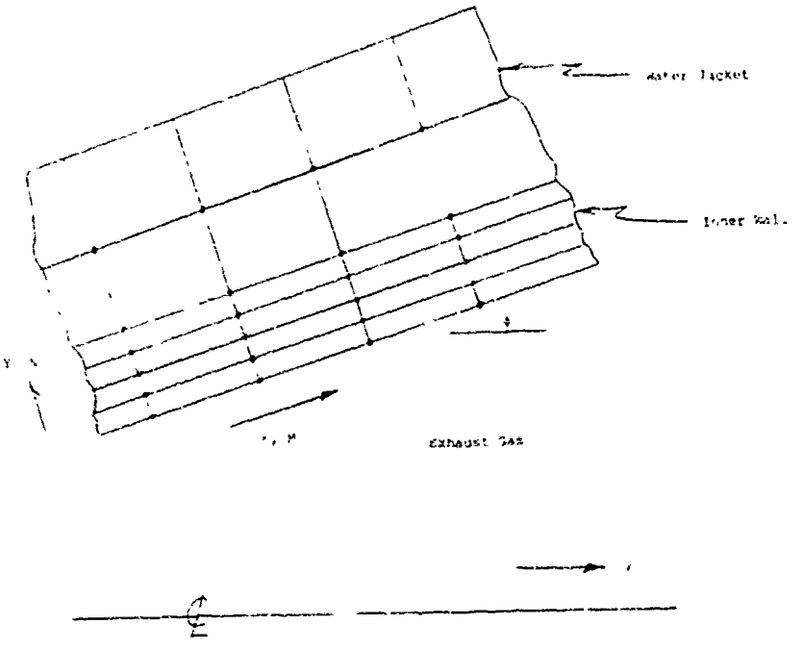

Figure 3. Finite Difference Grid System.

Equation 1 is formulated in explicit form using central difference approximations for the spatial derivatives and a forward difference approximation for the temporal derivative. This gives rise to

$$(T_{m-1,n} - 2\,T_{m,n} + T_{m+1,n})/(\Delta x)^2$$

$$+ \quad (T_{m,n-1} - 2\,Tm,n + T_{m,n+1})/(\Delta Y)^2$$

$$= \quad (\rho C/k)(T^{+}_{m,n} - T_{m,n}) \;/\; \Delta t \qquad (15)$$

where the superscript + indicates a temperature occurring at time (t + Δ t). Equation 15 may be solved for $T^{+}_{m,n}$ and written as

$$T^{+}_{m,n} = (T_{m,n-1} + T_{m,n+1} + Z^2(T_{m-1,n} + T_{m+1,n})$$

$$+ \quad (Ml - 2 - 2\,Z^2)\,T_{m,n}) \,/\, Ml \qquad (16)$$

where

$$Z = (\Delta Y/\Delta X)\,\cos\,\emptyset$$

and

$$Ml = \rho C(\Delta Y)^2/k\Delta t.$$

In this form the temperature distribution at time (t + t) may be solved for point by point in terms of a known temperature distribution at time t. This explicit formulation has the stability requirement that

$$Ml - 2 - 2\,Z^2 \geq 0$$

For a given ΔX and ΔY this places an upper bound on Δt but has presented no problems to date.

Equation 16 is applicable to all internal nodes. However, the first radial node (m,1) and the last radial node (m,L) involve boundary conditions and must be handled separately. In the case of these two nodes it is convenient to forsake the mathematical elegance of finite difference forms and to perform an energy balance on the element. Note that in terms of thermal capacity each of these nodes involves only one half an element. Written in explicit for node m,1 this takes on the following form:

$$h_m \Delta X(TAW_m - T_{m,1}) + (k\Delta Y/2\Delta X)\,(T_{m-1,1} - T_{m,1})$$

$$+ \quad (k\Delta Y/2\Delta X)\,(T_{m+1,1} - T_{m,1}) + (k\Delta X/\Delta Y)\,(T_{m,2} - T_{m,1})$$

$$+ \quad QPR_m \Delta X\,(TP_m - T_{m,1}) + QPI_m \Delta X + QPR_m \Delta X$$

$$= \quad (\rho C\Delta X\Delta Y/2\Delta t)(T^{+}_{m,1} - T_{m,1}) \qquad (17)$$

where h is the gas side film coefficient, TAW is the adiabatic wall temperature of the gas, QPT is the thermal energy flux per unit area caused by particle impingement, QPI is the inertial energy flux per unit area caused by particle impingement, and QPR is the radiant energy flux per unit area from the particles. Equation 17 may be solved for $T^+_{m,1}$ and written as

$$T^+_{m,1} = 2T_{m,2} + Z^2(T_{m-1,1} + T_{m+1,1}) + 2N1TAW_m$$

$$+ (2QPT_m \Delta Y/k)\, TP_m + (2\Delta Y/k)(QPI_m + QPR_m)$$

$$+ (M1 - 2 - 2Z^2 - 2N1 - 2QPT_m \Delta Y/k)\, T_{m,1})/M1 \qquad (18)$$

where

$$N1 = h\Delta Y/k.$$

Here as with Equation 16, one has the simplicity of an explicit formulation but the stability restriction that

$$M1 - 2 - 2Z^2 - 2N1 - 2QPT_m \Delta Y/k \geq 0$$

which places a slightly smaller upper limit on Δt than was associated with Equation 16.

Node m,L may be handled in the same fashion as node m,1 and results in

$$T^+_{m,L} = (2\, T_{m,L-1} + Z^2(T_{m-1,L} + T_{m+1,L}) + 2N2TC_m \qquad (19)$$

$$+ (M1 - 2 - 2Z^2 - 2N2)\, T_{m,L}) \,/\, M1$$

where TC is the local coolant temperature and N2 is identical to N1 only based upon the water side film coefficient. In this case stability requires that

$$M1 - 2 - 2Z^2 - 2N2 \geq 0$$

which places an additional upper bound on Δt.

An attempt to handle Equation 2 in the same fashion as Equation 1, that is to say, using a central difference approximation for the spatial derivative and a forward difference approximation for the temporal derivative will lead to numerical instability. On the other hand, using a backward difference approximation for the spatial derivative will lead to a stable formulation. Using this latter approach, Equation 2 may be approximated by

$$U_m (TC_m - TC_{m-1})/\Delta X + (2\pi R_m h_m/\rho CA_m)(TC_m - T_{m,L})$$

$$= -(TC_m^+ - TC_m)/\Delta t$$

Solving for TC_m^+

$$TC_m^+ = [TC_{m-1} + N3\ T_{m,L} + (M2 - 1 - N3)\ TC_m] / M2 \qquad (20)$$

where

$$M2 = \Delta X/U_m \Delta t = \rho A_m \Delta X / \dot{m} \Delta t \cos \phi$$

and

$$N3 = 2\pi R_m h_m \Delta X / \dot{m} C \cos \phi$$

and $\dot{m}$ is the mass flow rate of the coolant. Stability will require that

$$M2 - 1 - N3 \geq 0$$

and place yet another upper bound on Δt.

4. IMPLEMENTATION OF DHT

The following discussion is intended to be an overview of the code. Detailed discussion of the input and output will appear separately.

Prior to executing DHT, SSP must be run for the rocket motor and SCIPPY must be run for the diffuser. In running SPP it is necessary to save and catalog the exit plane information contained on TAPE29. This information and a small amount of hand input data is required by SCIPPY. In running SCIPPY it is necessary to catalog and save the data contained in TAPE99. Data contained in this file includes the diffuser geometry along with the edge conditions required for the evaluation of the heat loads on the diffuser.

Units for input data are selected on the basis of user convenience and are converted internally to pounds force, feet, seconds, degrees Rankine, and pounds mass. Units for output are selected on the basis of user convenience.

The edge condition data provided by SCIPPY on TAPE99 are randomly spaced along the axis of the diffuser. Since the numerical analysis within DHT assumes a uniformly spaced grid system, the first major operation within DHT is to read the SCIPPY tape and to interpolate within the data to create a set of uniformly spaced edge conditions. In conjunction with this manipulation, all edge condition type calculations within the DHT model are also performed. These include the calculation of particle impingement mass flux, debris layer data, and particle related heat fluxes. In as much as neither the rocket motor chamber pressure nor the test cell pressure remain constant throughout the test, provision is made to update the edge conditions by way of additional SCIPPY tapes. This provision is handled through the index SCIPPY and numbered data sets identified as SCIP(1) through SCIP(SCIPPY).

Once the edge conditions have been established, DHT prepares to call TBL in order to obtain the gas side film coefficients and adiabatic wall temperatures of the gas. The input data has included a value for the film coefficient at the point of plume impigement, obtained from Equation 6 and adjusted by an augmentation factor. It is necessary for DHT to establish values for the boundary layer thicknesses at the point of plume impingement such that TBL will predict this value for the impingement point film coefficient. DHT will accept a user selected initial trial value for the

energy thickness, hold the momentum thickness equal to a user selected constant times the energy thickness, and iterate to seek a set of momentum and energy thicknesses that will result in the desired impingement point film coefficient. At best, this is no more than a means to an end. It will, however, result in an impingement point heat flux in keeping with a known correlation. There is no reason to expect this to predict valid film coefficient data immediately downstream of impingement but hopefully local edge conditions will dominate and produce valid results further downstream. The validity of this approach will have to be reviewed as experimental data become available. Since the film coefficients predicted by TBL are mild functions of the gas side surface temperatures, provision is made through the parameters ICALL and DCALL to update the film coefficients as the temperature of the diffuser wall rises. The code has an initial update built in to it that occurs ten time increments into the calculations. Subsequent to this, an update occurs every DCALL time increments or with each new set of edge conditions obtained by way of a SCIPPY tape. TBL is a time consuming code and indiscriminate updating should be avoided. To date it has been adequate to update TBL just prior to the final output and verify that no significant changes have occured in the film coefficients.

Many of the coefficients within the governing equations are independent of temperature and are evaluated as preliminary calculations. Much of this information is output as a matter of convenience to the user.

The output that occurs at time zero or following the reading of a new SCIPPY tape is quite extensive and contains a great deal of boundary layer, debris layer, and individual heat flux information that will remain constant throughout the calculations. Future output will occur every DOUT time increments and is appreciably more abbreviated.

If the parameter DAFLAG has been read in as other than zero, DHT has the capability to store gas side wall temperature, water side wall temperature, coolant temperature as functions of either time or position for future use in creating graphic information. Unless this option is implemented, temperatures are stored for time t and (t + Δ t) only. A more extensive discussion of the option is contained under the separate heading of GRAPHIC OUTPUT.

The main heat transfer calculation is an implementation of the finite difference equations presented earlier in Section 3. It is in order to

comment on the handling of the end conditions. The near end and far end of the diffuser wall are treated as adiabatic planes. These conditions are implemented by extending the grid system one grid line beyond each end and step by step assigning the outboard nodes mirror image values from internal nodes. This allows nodes on the two end planes to be handled as though they were internal nodes and introduces no additional equations. The coolant temperature at the inlet plane of the diffuser is held at the supply temperature and the upstream differencing used within Equation 20 requires no knowledge of coolant temperature beyond the exit plane of the diffuser.

Following each time step there is the opportunity to output the temperature distribution through the parameter DOUT, to store a portion of the temperature data under the DAFLAG option, to update the gas side film coefficients under the DCALL option, and to update the edge conditions with a new SCIPPY tape. Independent of any of the above mentioned options, the water side film coefficients are a function of the average film temperatures and are updated following each time step.

5. GRAPHIC OUTPUT

Provision is made for saving data sets for use with the Tektronics EZGRAF graphics system. This option is implemented by setting the flag DAFLAG to any nonzero integer. Data sets will be written to TAPE99. The first data set written will be a set of axial locations measured in inches and locating grid lines on an index interval of DXBA. Following this data set will be a series of three data sets, each consisting of a single time followed by a set of gas side wall temperatures, water side wall temperatures, or coolant temperatures occurring at axial locations consistent with the initial set of axial location data. A series of three such data sets will be written on the same time interval as the printed output from the code. The next data set written will be a time base for displaying temperature as a function of time. A sequence of times will be written on a time interval of DDAOUT time steps. This time base is followed by a series of data sets consisting of a single axial location followed gas side wall temperatures, water side wall temperatures, or coolant temperatures on the above mentioned time interval. As many as five axial locations for such temperature sets may be selected by specifying the axial grid index MDATA. All data sets, with the exception of axial position and time, are written in rounded integer form because of the real number storage limitations within EZGRAPF. Axial position and time are retained in real number form.

6. INPUT INFORMATION

6.1 Nomenclature

Variable	Description	Type
ACN	Accommodation coefficient, kinetic energy normal to the diffuser wall (none)	Real
ACP	Accommodation coefficient, kinetic energy parallel to the diffuser wall (none)	Real
ACT	Accommodation coefficient, thermal energy (none)	Real
ATHETA	Proportionality constant (none) THETAI = ATHETA * PHII	Real
DAFLAG	Flag. Data sets for graphic output are stored if DAFLAG is nonzero. (none)	Integer
DCALL	Frequency of TBL update, every DCALL time steps (none)	Integer
DDAOUT	Frequency with which temperature is saved for graphic output as a function of time, every DDAOUT time steps (none)	Integer
DISCH	Volumetric flow rate of coolant (gpm)	Real
DMXBA	Frequency with which temperature is saved for graphic output as a function of time, every DMXBA grid lines (none)	Integer
DOUT	Frequency of printed output, every DOUT time steps (none)	Integer
DX	Axial step size (inches)	Real
DXMAX	Maximum allowable axial step size within TBL (inches)	Real
DTAU	Time step size (sec)	Real
ENDTBL(K)	Last time step for which the Kth SCIPPY tape should be used (none)	Integer
GAMO	Stagnation ratio of specific heats associated with the Kth SCIPPY tape (none)	Integer
HIMPK(K)	Gas phase heat transfer coefficient at the point of plume attachment associated the Kth SCIPPY tape ($B/sec\text{-}ft^2\text{-}R$)	Real

Variable	Description	Type
HT	Radial height of the water jacket passage (inches)	Real
KRPIK(K)	Radiation source strength associated with the Kth SCIPPY tape (B/sec-ft)	Real
KW	Thermal conductivity of the diffuser wall (B/sec-ft-R)	Real
MDATA(N)	Axial grid location at which temperature is to be saved for graphic output (none)	Integer
MU	Dynamic viscosity of the coolant (lbm/ft-sec)	Real
NCH	Number of coolant channels (none)	Integer
NDATA	Number of axial positions MDATA(N) at which temperatures are to be saved for graphic output (none)	Integer
NDTAU	Number of time steps of numerical analysis to be performed (none)	Integer
NDY	Number of diffuser wall elements taken radially (none)	Integer
NSCIP	Number of SCIPPY tapes to be read (none)	Integer
PHII	Initial estimate of the energy thickness at the point of plume attachment (feet)	Real
PRK(K)	Stagnation Prandtl Number associated with the Kth SCIPPY tape (none)	Real
RBARK(K)	Gas constant associated with the Kth SCIPPY tape (ft-lbf/lbm-R)	Real
RHOC	Mass density of the coolant (lbm/ft^3)	Real
RHOW	Mass density of the diffuser wall (lbm/ft^3)	Real
SCIP(K)	Identifier. Various SCIPPY tapes may be attached as TAPEnn. SCIP(K) is the two digit identifier nn. Provision is made within the DHT program card for TAPE11 and TAPE12. This may be expanded if the user desires and has the storage space available. (none)	Integer
SPHTC	Specific heat of the coolant (B/lbm-R)	Real
SPHTW	Specific heat of the diffuser wall (B/lbm-R)	Real

Variable	Description	Type
TI	Initial temperature (^{o}R)	Real
TKW	Thickness of the diffuser inner wall (inches)	Real
TOK(K)	Stagnation temperature associated with the Kth SCIPPY tape (^{o}R)	Real
TYPACH	Type ACN TYPACN ≠ 0, ACN = ACN TYPACN = 0, ACN = 0.8 SIN B (none)	Integer
TYPDBR	Type debris layer analysis TYPDBR = 0, effects of model excluded TYPDBR = 0, effects of model included Parameters will be calculated and outputted regardless of the value of TYPDBR (none)	Integer
XMOTOR	Distance from the motor exit plane to the diffuser inlet plane. If the exit cone of the motor extends into the diffuser, XMOTOR will be negative. (inches)	Real
XSTOP	Extent of diffuser to be analyzed as measured from the inlet plane of the diffuser (inches)	Real
WIDTH	Width of each coolant channel (inches)	Real
ZMOUK(K)	Stagnation viscosity associated with the Kth SCIPPY tape (lbm/ft-sec)	
ZMVISK(K)	Exponent associated with the Kth SCIPPY tape viscosity vs temperature model ZMVISK = ZMOUK (T/TOK) (none)	Integer

6.2 INPUT PROCEDURES

DHT receives its input in the form of a series of data card images available as TAPE5. Shown below is a card by card description of the format and data contained within each card image.

CARD 1 (12A6)
TITLE FOR THE ANALYSIS

CARD 2 (8F10.4)
DX, DTAU, DXMAX

CARD 3 (8I10)
NDTAU, NDY, NCH, DOUT, DCALL, NSCIP

CARD 4 (8I10)
DAFLAG, DDAOUT, DMXPA, NDATA, MDATA(1), -----, MDATA(NDATA)

If no data sets are to be stored for grephic output, this card image may be left blank but must be included.

CARD 5 (8F10.4)
TKW, WIDTH, HT

CARD 6 (8F10.4)
RHOW, RHOC, SPHTW, KW, MU

CARD 7 (8F10.4)
DISCH, XMOTOR, XSTOP, TI

CARD 8 (8F10.4)
ACN, ACP, ACT

CARD 9 (8I10)
TYPACN, TYPDBR

CARD 10 (8I10)
SCIP(1), -----, SCIP(NSCIP)

CARD 11 (8I10)
ENDTBL(1), -----, ENDTBL(NSCIP)

CARD 12 (8F10.4)
TOK(1), -----, TOK(NSCIP)

CARD 13 (8F10.4)
RBARK(1), -----, RBARK(NSCIP)

CARD 14 (8F10.4)
PRK(1), -----, PRK(NSCIP)

CARD 15 (8F10.4)
ZMUOK(1), -----, ZMUOK(NSCIP)

CARD 16 (8F10.4)
ZMVISK(1), -----, ZMVISK(SCIP)

CARD 17 (8F10.4)
GAMOK(1), -----, GAMOK(NSCIP)

CARD 18 (8F10.4)
KRPIK(1), -----, KRPIK(NSCIP)

CARD 19 (8F10.4)
HIMPK(1), -----, HIMPK(NSCIP)

CARD 20 (8F10.4)
PHII, ATHETA

6.3 INPUT GUIDELINES

ATHETA, PHII.

PHII is the first trial value of the energy thickness used by the iterative procedure that seeks initial energy and momentum thicknesses consistent with the desired impingement point heat transfer coefficient. A value of PHII that is either too large or too small will cause TBL to fail. PHII equal to 0.005 feet has been found to be successful with the motors considered to date. ATHETA is the ratio of the momentum thickness to the energy thickness and is used only in the iterative procedure. A value of 1.1 has been found to be successful with the motors considered to date. A value of 1.0 has often caused TBL to fail.

NSCIP, SCIP (K).

For simple analyses the flow field within the diffuser will be assumed to remain constant with respect to time and NSCIP will be 1. If, on the other hand, either the chamber pressure of the motor or the test cell pressure change significantly during burn time, it may be desirable to account for the resulting changes in the diffuser flow field. This would require the use of two or more SPP and SCIPPY runs and would generate two or more SCIPPY tapes. If, for example, the flow conditions were quite similar during the early and late portions of the burn time but differed significantly during the middle of the burn time, one could consider using two SCIPPY runs. NSCIP would be read in as 3. The two SCIPPY tapes could be attached as TAPE11 and TAPE12. SCIP(1) would be read in as 11, SCIP(2) would be read in as 12, and SCIP(3) would be read in as 11. ENTBL(1), ENTBL(2), and ENDTBL(3) would indicate the last time step for which each set of data would be used. Cards 12 through 19 will contain NSCIP entries. If, as in the example just cited, a given tape is to be used more than one time, there will be duplication among the entries but there will be NSCIP entries per card. Provision has been made in the program card for TAPE11 and TAPE12. The user may expand on this as machine time and space permit. The program is dimensioned to allow NSCIP to be as large as 10.

HIMPK(K), XRPIK(K).

See sample problems for details on calculating these parameters.

7. OUTPUT INFORMATION

7.1 Nomenclature

Variable	Description
A	Cross-sectional area of the water jacket normal to the diffuser axis (ft^2)
C1	N1 = C1 x HG(M) ($B/sec-ft^2-R)^{-1}$ (See Equation 18)
	N2 = C1 x HC(M) ($B/sec-ft^2-R)^{-1}$ (See Equation 19)
C2	N. = C2 x HC(M) ($B/sec-ft^2-R)^{-1}$ (See Equation 20)
DEBRIS(J)	Mass flow rate of the particle group J within the debris layer (lbm/sec)
DEBRIS FACTOR	(See Equation 11A)
DELTA	Velocity boundary layer thickness (inches)
DP(J)	Particle diameter for group J (microns)
HC	Water side heat transfer coefficient ($B/sec-ft^2-R$)
HG	Gas side heat transfer coefficient ($B/sec-ft^2-R$)
HG(1)	Gas side heat transfer coefficient at the point of initial plume impingement, as generated by TBL ($B/sec-ft^2-R$)
HIMPK(K)	Gas side heat transfer coefficient at the point of initial plume impingement, as specified by the input data and associated with the Kth SCIPPY tape ($B/sec-ft^2-R$)
KRPIK(K)	Particle radiation source strength associated with the Kth SCIPPY tape (B/sec-ft)
M	Axial grid location, M = 2 indicates the diffuser inlet (none)
MDOT(J)	Mass flow rate of particle group J impinging upon the wall in the absence of debris layer effects ($lbm/sec-ft^2$)
M1	(See Equation 16) (none)
M2	(See Equation 20) (none)

Variable	Description
PHII	Energy boundary layer thickness at the point of plume impingement (ft)
QHC	Water side convective heat flux (B/sec-ft^2)
QHG	Gas side convective heat flux (B/sec-ft^2)
QPI	Inertial heat flux associated with particle impingement (B/sec-ft^2)
QPIJ(J)	Inertial heat flux associated with particle impingement, group J only (B/sec-ft^2)
QPR	Heat flux associated with particle radiation (B/sec-ft^2)
QPT	Thermal heat flux associated with particle impingement (B/sec-ft^2)
RE	Reynolds Number for the coolant flow (none)
R	Local diffuser radius (feet)
R1	Local inner radius of the water jacket (feet)
R2	Local outer radius of the water jacket (feet)
SCIPPY	The number of the SCIPPY tape being used (none)
SINEJ(J)	Sine of the impingement angle with which particle group J strikes the diffuser wall (none)
TAW	Adiabatic wall temperature of the edge condition gas flow ($^{\circ}$R)
V	Coolant velocity (fps)
X	Axial location measured from the inlet plane of the diffuser (inches)
Y	Diffuser inside radius (feet)

7.2 GENERAL DESCRIPTION

The output from DHT is well labelled and with the above nomenclature should be self-explanatory; however, a general description of the output should be useful to the first time user.

The initial set of information generated by DHT consists of a user defined title for the analysis followed by a listing of the input data supplied by the user.

At this point DHT will read and organize the data contained on the SCIPPY tape and will then call TBL. The next several sets of output information from DHT will actually be generated from within TBL. The first of these sets of information will be a set of boundary layer parameters. This will be followed by a set of geometry data (radius vs axial location) for the diffuser, freestream Mach number, and gas side wall temperature for the diffuser. Following this will be a set of freestream pressure, temperature, velocity, and density data for use in the boundary layer analysis. At this point the listing will only show data for the first four axial stations following the point of plume impingement. This is caused by the fact that DHT is at this point setting up to begin an iterative routine for selecting starting values for the momentum and energy boundary layer thickness that will result in TBL matching a user supplied heat transfer coefficient at the point of plume impingement. DHT will at this point output a series of sets of PHII, HG(1), and HIMPK that will allow the user to observe the process by which DHT will select the starting boundary layer thicknesses. Once this process is complete, DHT will call TBL and generate boundary layer information for the entire diffuser. This will generate as output a new set of boundary layer parameters that will include the selected starting boundary layer thicknesses followed by a complete listing of diffuser wall geometry and edge conditions.

At this point DHT will perform a number of preliminary calculations and output preliminary data that will include M1, RE, V, HC1, C1, SCIPPY, KRPIK, DP(K), R(M), R1, R2, A, M2, and C2. During the listing of this information, DHT will perform a check on the various stability criteria and print a warning message if any are being violated.

DHT is now ready to begin the main heat transfer analysis. The initial condition listing that appears at this point is quite comprehensive and includes numerous parameters that will remain constant throughout the entire analysis or at least until a new SCIPPY tape is read in. Information will be listed at every axial station and will include X, MDOT, SINE, DEBRIS, DEBRIS FACTOR, MDOTW, QPIJ, DELTA, HG, QHG, QPI, QPT, QPR, QHC, TAW, T, and TC. It should be noted that the wall temperatures are labelled as WALL and are listed sequentially from the gas side wall temperature to the water side wall temperature. Following this initial listing the frequency of output is controlled by the parameter DOUT and is appreciably abbreviated unless a new SCIPPY tape is read in which case the more comprehensive listing is triggered.

8. SAMPLE PROBLEM

8.1 GENERAL

DHT has been used to analyze two Super BATES firings conducted at the AFRPL Test Area 1-42 and to provide predictions for a proposed Minuteman III Stage 3 firing in the same facility. The necessary input data for the January 13, 1983 Super BATES firing will be presented here along with the DHT predictions for all three firings.

8.2 Preliminary Calculations

Most of the input information required by DHT is available from the statement of the problem or the output from SPP or SCIPPY. There are, however, two items that are left as preliminary hand calculations. The impingement point heat transfer coefficient must be evaluated from Equation 6 with the free stream velocity gradient approximated from the edge condition information contained in the SCIPPY tape.

$$h = k\sqrt{Pr(dU/ds)/2\nu}$$

$k = 4.58 \times 10^{-5}$ B/sec-ft-^{o}R

$Pr = 0.4547$

$dU/ds = 1006$ sec

$\nu = 0.0452$ ft^2/sec

$h = 0.00326$ B/sec-ft^2-^{o}R

Equation 6 is a laminar correlation and must be multiplied by an augmentation factor which for the moment remains unknown. It is hoped that as experimental diffuser data become available this factor will become better defined but for the moment a figure of 2.5 is viewed as a conservative estimate and leads to:

HIMPK = 0.0082 B/sec-ft^2-^{o}R

The radiation source strength KRPI must be evaluated using Equation 5. The information necessary to make this calculation is obtained from the output of SPP. SPP partitions the mass flow of particles into three particle groups based upon diameter. These three particle groups each carry the same mass flow rate. Given the uncertainty surrounding the particle flow field, the simplistic radiation model being used, and the relative size of the radiation heat flux, it seems appropriate to evaluate this source strength for the

middle size particle group and to multiply this figure by three. At such a time as the particle flow is better understood it would be appropriate to revise not only this procedure but the radiation model.

$$q = \dot{m}_p \sigma \varepsilon T_p / U_p \rho_p R_p$$

$$m_p = 16.72 \text{ lbm/sec}$$

$$U_p = 8556 \text{ fps}$$

$$T_p = 4189 \ ^{\circ}R$$

$$\rho_p = 248 \text{ lbm/ft}^3$$

$$\sigma = 0.1714 \times 10^{-8} \text{ B/hr-ft}^2\text{-}^{\circ}R^4$$

$$\varepsilon = 0.25$$

$$R_p = 9.829 \times 10^{-6} \text{ ft}$$

$$q = 88 \text{ B/sec-ft}$$

This figure is the source strength resulting from a single particle group and must be multiplied by three such that

KRPI = 264 B/sec-ft.

8.3. INPUT DATA

The following data is necessary in order to run the program.

DX = 1.0 in

DTAU = 0.05 sec

DXMAX = 1.0 in

NDTAU = 100 (this will provide 5 seconds of data)

NDY = 4

NCH = 4

DOUT = 20 (this will provide data every second)

DCALL = 90 (this will update TBL just prior to the end of the run)

NSCIP	= 1	(this provides for using only one SCIPPY tape)
DAFLAG	= 1	(set equal to non-zero this will provide for the ring of data sets for use with graphic output)
DDAOUT	= 20	(data will be saved every second)
DMXBA	= 1	(data will be saved every inch)
NDATA	= 5	(data will be saved as a function of time at five axial locations)
MDATA(N)	= 22, 23, 24, 25, 26	(data will be stored as a function of time at 20, 21, 22, 23, and 24 inches)
TKW	= 0.5 in	
WIDTH	= 5.25 in	
HT	= 2.75 in	
RHOW	= 490 lbm/ft^3	
RHOC	= 62.4 lbm/ft^3	
SPHTW	= 0.1 B/lbm-$^\circ$R	
SPHTC	= 1.0 B/lbm-$^\circ$R	
KW	= 0.00863 B/sec-ft-$^\circ$R	
MU	= 0.000759 lbm/ft-sec	
DISCH	= 1100 gpm	
XMOTOR	= 12 in	(the exit plane of the motor is positioned 12 inches in front of the inlet to the diffuser)
XSTOP	= 52 in	(the calculation must be terminated at 52 inches because SCIPPY fails at this point for a motor with an exit plane diameter as small as Super BATES in a diffuser as large as this)
TI	= 510°R	
ACN	= 1.0	

ACP = 0.0

ACT = 0.0

TYPACN = 0

TYPDBR = 0

SCIP(N) = 11 (if more than one SCIPPY tape is to be called this will be a sequence of tape numbers)

ENDTBL(N) = 100

TOK(N) = 6666^{o}R

RBARK(N) = 80.13 ft-lb/lbm-^{o}R

PRK(N) = 0.4547

ZMUOK(N) = 0.00006241 lbm/ft-sec

ZMVISK(N) = 0.656

GAMOK(N) = 1.29

KRPIK(N) = 264 B/sec-ft

HIMPK(N) = 0.0082 B/sec-ft-^{o}R

PHII = 0.005 ft

ATHETA = 1.1

8.4 EXECUTION OF THE PROGRAM

At the time of execution, the above data must be available to DHT as TAPE5 and in a format as specified in Section 6. Listed is a set of such card images consistent with the above data.

```
CARD 1
SUPER BATES - 13JAN83

CARD 2
1.0     0.05    1.0

CARD 3
100     4       4       20      90      1

CARD 4
1       20      1       5       22      23      24      25      26
```

CARD 5
0.5 5.25 2.75

CARD 6
490.0 62.4 0.' 1.0 0.00863 0.000759

CARD 7
1100.0 12.0 52.0 510.0

CARD 8
1.0 0.0 0.0

CARD 9
0 0

CARD 10
11

CARD 11
100

CARD 12
6666.0

CARD 13
80.13

CARD 14
0.4547

CARD 15
0.00006241

CARD 16
0.656

CARD 17
1.29

CARD 18
264.0

CARD 19
0.0082

CARD 20
0.005 1.1

8.5 RESULTS

Output generated by DHT and based on these data is presented in Figures 4 and 5. The 77-inch diffuser located in Test Area 1-42 is instrumented to record water side wall temperatures on roughly 2-inch centers for the first 6 feet of the diffuser. The diffuser is also instrumented to record coolant temperatures on roughly the same intervals, but the burn time of the Super BATES motor is only about 5 seconds and does not result in an appreciable rise in the coolant temperature. It is unfortunate that SCIPPY fails after the first 52 inches of the diffuser but up until that point it would appear that the output from DHT tracks the experimental data quite well.

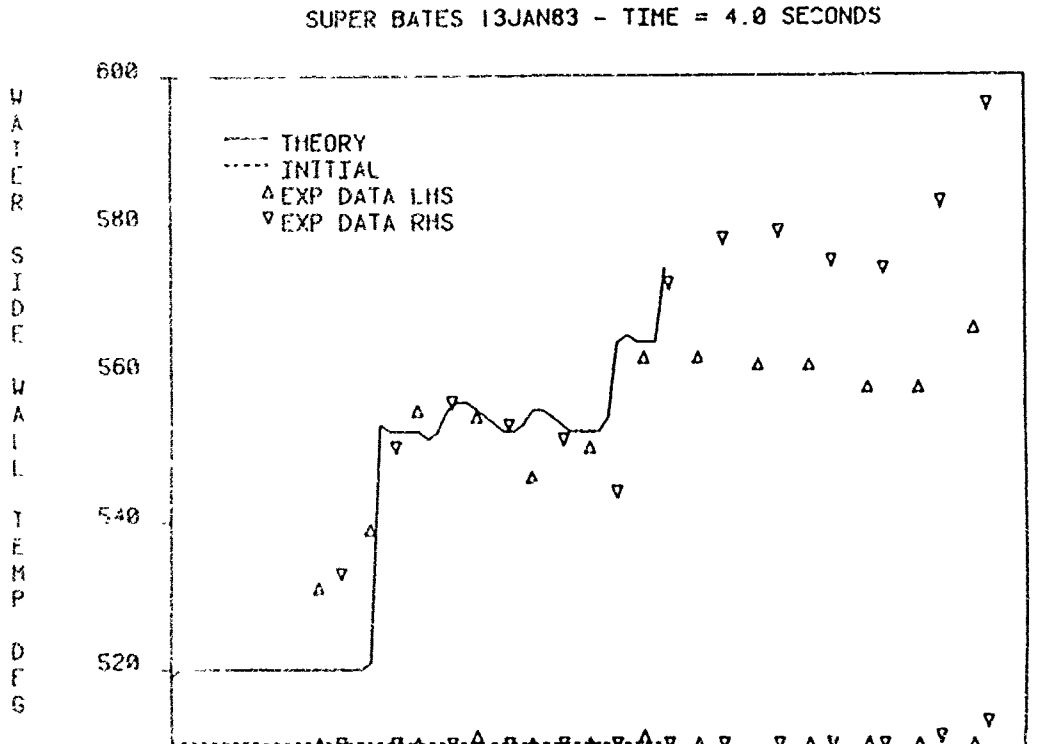

Figure 4. Axial Temperature Variations.

Figure 4 shows the axial temperature variations of the water side wall temperature at approximately the end of the burn time. Unfortunately SCIPPY breaks down prior to the point at which there is any particle impingement upon the diffuser wall. Therefore the correlation between DHT and the experimental data seen in Fig. 4 in no way validates the manner in which the code is handling particle interactions with the wall. It does, however, lend support to the manner in which the code is handling the point of plume impingement.

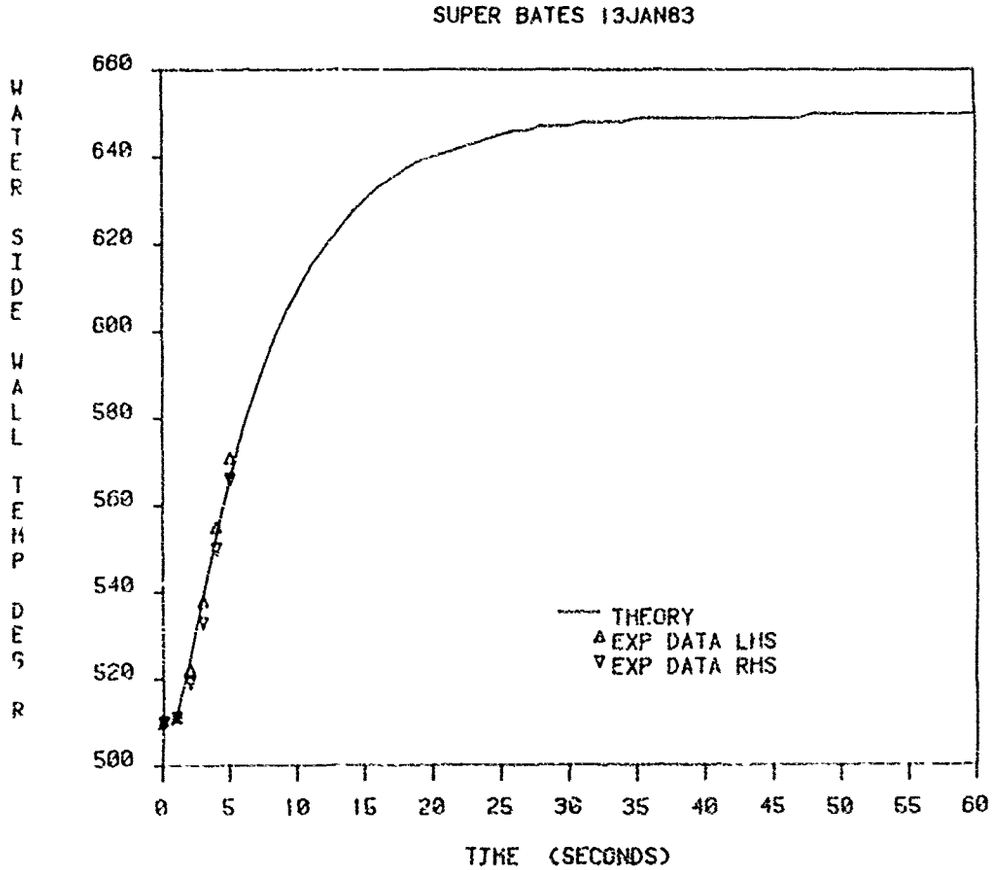

Figure 5. Water Side Wall Temperature as a Function of Time in the Vicinity of Plume Impingement.

Figure 5 shows the water side wall temperature as a function of time in the vicinity of plume impingement. Here again the degree with which the predictions of DHT track the experimental data is very gratifying, but the burn time of the Super BATES motor is insufficient to show whether the predictions and the experimental data will compare favorably at burn times approaching 60 seconds. Until data are available for a motor with a burn time approaching at least 30 seconds, it will be impossible to do much in terms of validating the predictions of DHT. Also, until a motor which SCIPPY can handle is tested or until a better version of SCIPPY is available, very little can be said as to how well DHT handles the particle wall interactions.

Several comments are in order concerning the experimental data shown in Figure 4. The diffuser is instrumented to record water side wall temperature by means of thermocouples spot welded to the inner wall of the water jacket. The junctions are formed by spot welding each thermocouple lead to the wall individually and allowing the wall to become a portion of the thermocouple circuit. It was hoped that by so doing it would be possible to locate the effective junction at the surface of the diffuser wall. It is felt that the data seen in Fig. 4 stand in testimony to the success of this endeavor. These thermocouples are sited along two straight line paths along the axis of the diffuser. One of these paths labeled LHS is located roughly 45 degrees from the top and along the left hand side of the diffuser. The other path is roughly 45 degrees from the top and along the right hand side of the diffuser. The data shown in Figure 4 reveals a definite biasing of the data in terms of left vs right hand side but shows either set of data from a single side of the diffuser to be very self-consistent. This consistency among data from a single side of the diffuser is felt to rule out experimental scatter and to validate the quality of the data. The bias seen between the LHS and the RHS is definitely real. The exact same trend can be seen in data gathered from a December 3, 1982 test of a Super BATES motor and presented in Figure 1. This same trend was also seen in an entirely different motor tested in this facility prior to the December Super BATES firing. This left vs right variation in the data could be explained in terms of a lack of symmetry within the diffuser or the water jacket or a misalignment of the test stand with respect to the diffuser. For the moment, however, it is real and measurements taken on the facility reveal no misalignment of the test stand with respect to the diffuser.

To the extent possible at this time the data contained in Figs. 4 through 6 support the validity of both the code and the experimental data, however, there is a strong need for experimental data from a motor compatible with SCIPPY and having a burn time of 30 seconds or longer.

Figures 7 through 9 show predictions from DHT for a proposed Minuteman III Stage 3 test. Unfortunately this test has yet to be conducted and therefore there are no experimental data for comparison. The predictions are included as being indicative of the capability of the DHT code.

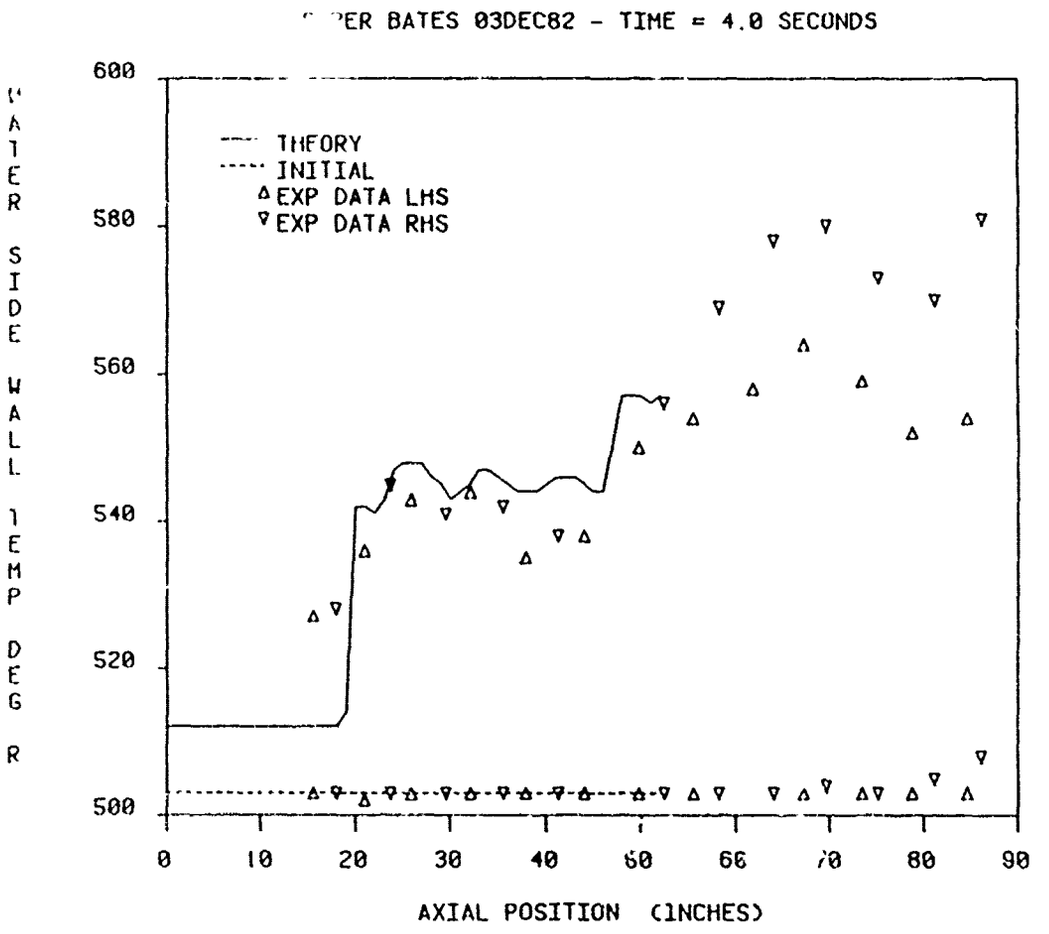

Figure 6. Data from December 3, 1982 Test of Super BATES Motor.

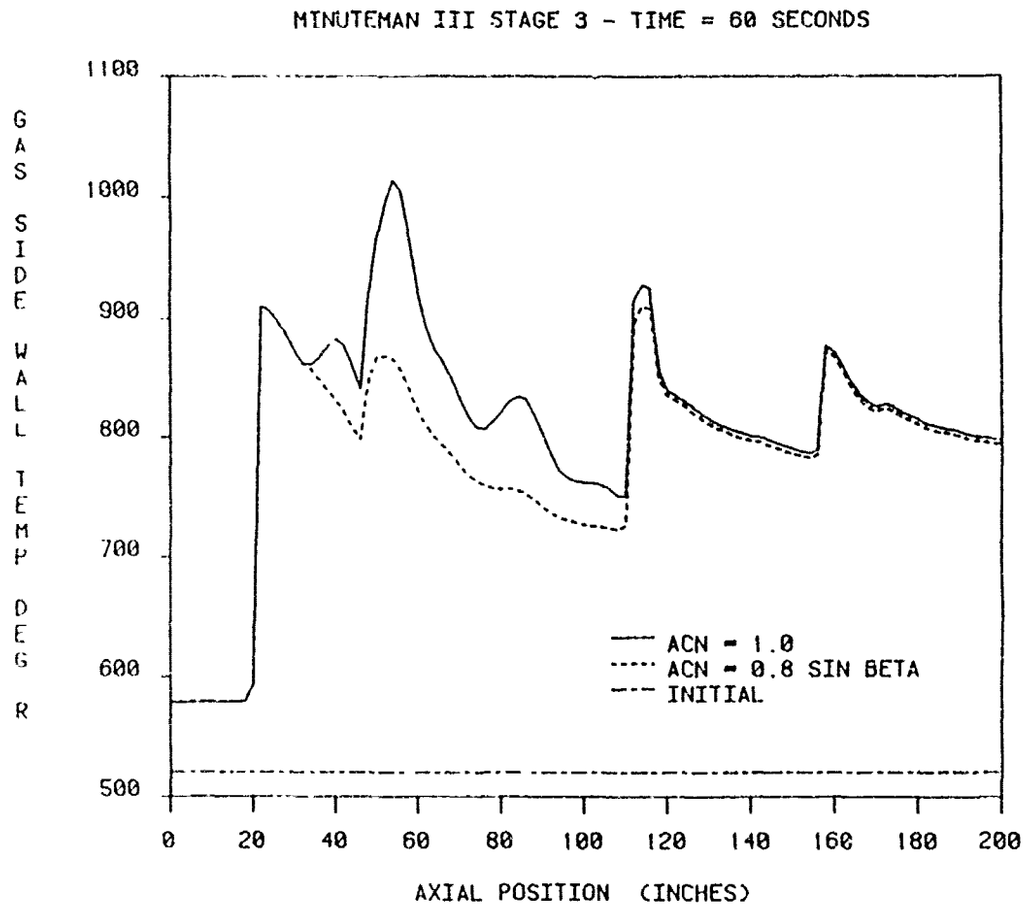

Figure 7. Predictions from DHT for Proposed Minuteman III Stage 3 Test.

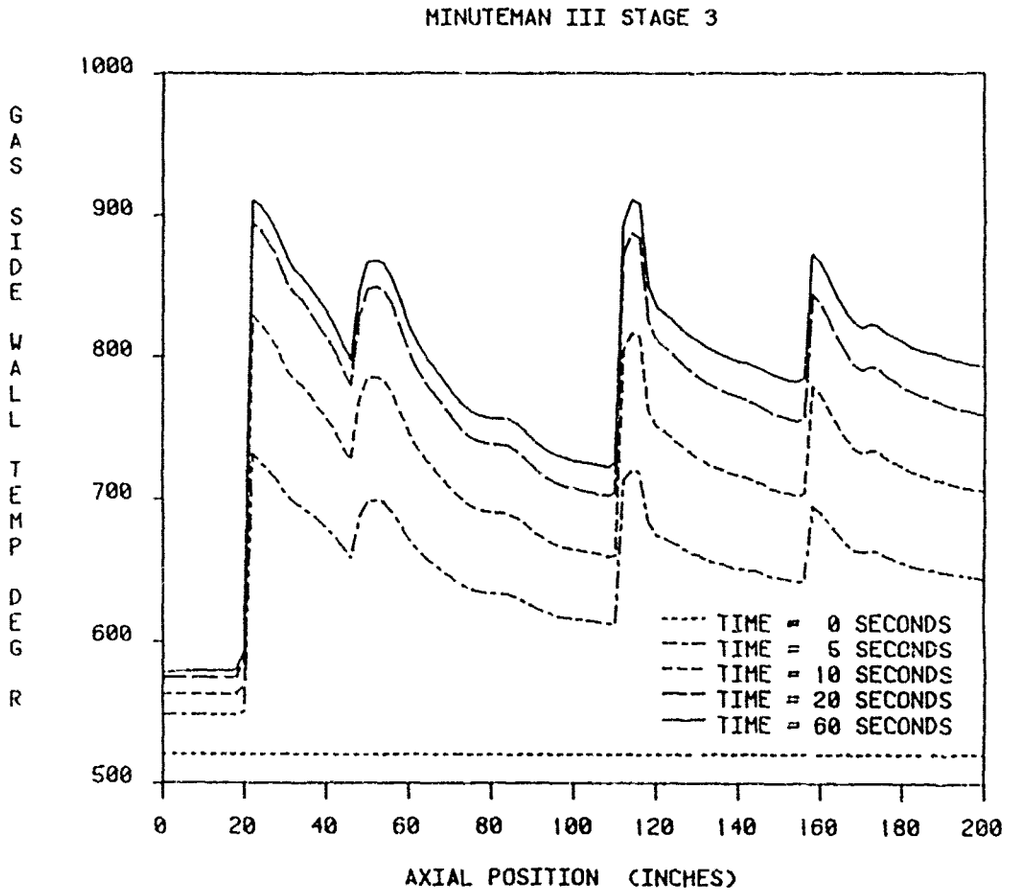

Figure 8. Predictions from DHT for Proposed Minuteman III Stage 3 Test.

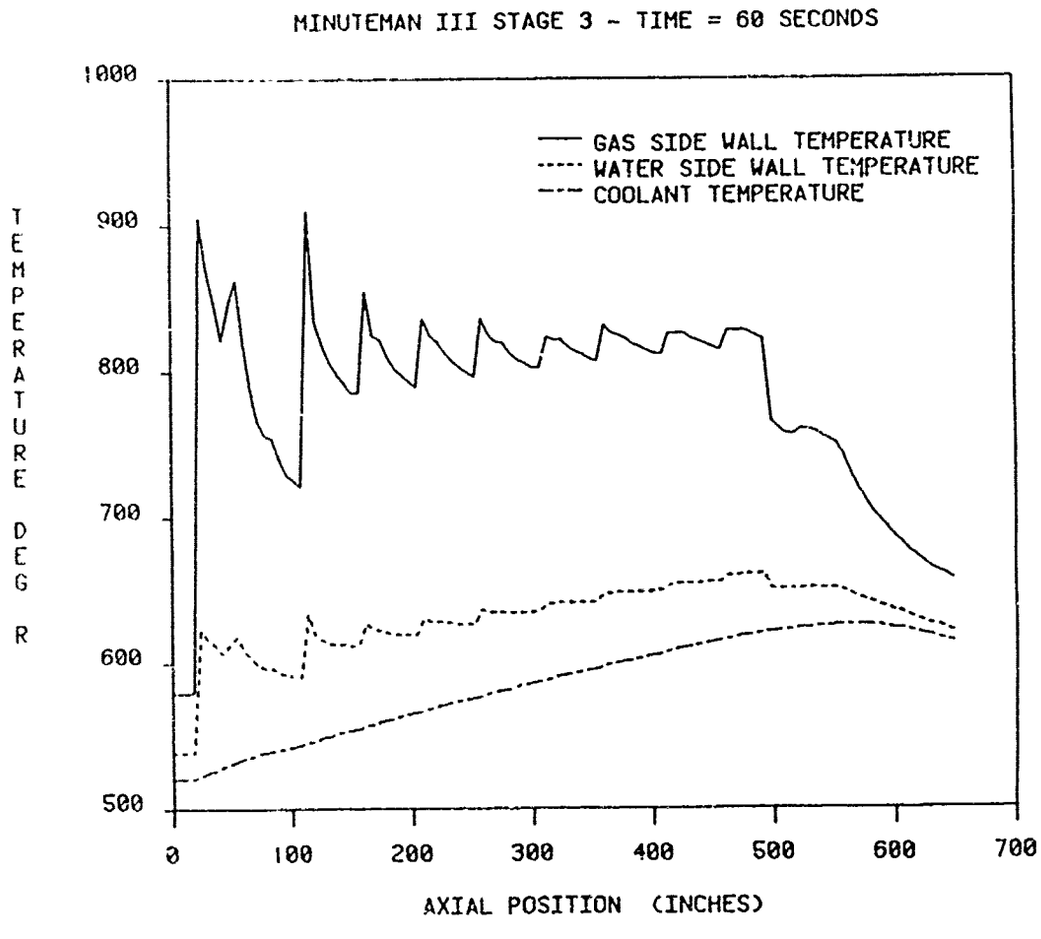

Figure 9. Predictions from DHT for Proposed Minuteman III Stage 3 Test.

REFERENCES

1. Trout, M. J. and McCay, T. D., "A Computational Model for Diffuser Heat Transfer Analysis," AIAA 16th Thermophysics Conference, Palo Alto, Calif, June 1981.

2. Pergament, H. S., Diffuser Heat Transfer Study, Final Report, Science Applications, Inc., Princeton, New Jersey, Redstone Arsenal Contract No. DAAHO1-M-0330, March 1981.

3. Kessel, P. A., unpublished report.

4. Nickerson, G. R., Coats, D. E., and Hermsen, R. H., Interim Technical Report, A Computer Program for the Prediction of Solid Propellant Rocket Motor Performance, Report No. AFRPL TR-80-34, Software and Engineering Associates, Inc., Santa Ana, Calif, and Chemical Systems Division-United Technologies, Sunnyvale, Calif, December 1980.

5. Dash, S. M., Pergament, H. S., Thorpe, R. D., Abuchowski, S. A., and Hussain, J. C., Operational Instructions for a Preliminary Version of the JANNAF Standard Plume Flowfield Model (SPF/1), Report No. ARAP 415, Aeronautical Research Associates of Princeton, Inc., Princeton, New Jersey, June 1980.

6. Dash, S. M., A Two-Phase Flow Version of SCIPPY for the Analysis of Supersonic Exhaust Plumes, Nozzles, and Diffusers, Report No. ARAP 426, Aeronautical Research Associates of Princeton, Inc., Princeton, New Jersey, September 1980.

7. Weingold, H. D., The ICRPG Turbulent Boundary Layer Reference Program, Pratt and Whitney Aircraft, East Hartford, Conn, July 1968.

8. Donaldson, C. duP., Snedeker, R. S., and Margolis, D. P., "A Study of Free Jet Impingement. Part 2. Free Jet Turbulent Structure and Impingement Heat Transfer," J. Fluid Mech., Vol. 45, Part 3, pp. 477-512, 1971.

9. Wickman, J. H., Mockenhaupt, J. D., and Ditore, M. J., "An Investigation of Particle Impingement in Solid Rocket Nozzles," AIAA/SAE/ASME 15th Joint Propulsion Conference, Las Vegas, Nev, June 1979.

10. Marks, L. S., Standard Handbook for Mechanical Engineers, 7th ed., McGraw-Hill Book Company, New York, 1967, Section 4.